


# T-type $\text{Ca}^{2+}$ channels play a dual role in modulating the excitability of dorsal root ganglia neurons

Molecular Pain  
Volume 18: 1–11  
© The Author(s) 2022  
Article reuse guidelines:  
[sagepub.com/journals-permissions](https://sagepub.com/journals-permissions)  
DOI: 10.1177/17448069221132224  
[journals.sagepub.com/home/mpx](https://journals.sagepub.com/home/mpx)  


Tong Zhu<sup>1,2</sup>  and Yuying Wang<sup>1,3,4</sup> 

## Abstract

A subgroup of low-threshold dorsal root ganglia (DRG) neurons discharge action potentials (APs) with an afterdepolarizing potential (ADP). The ADP is formed by T-type  $\text{Ca}^{2+}$  currents. It is known that T-type  $\text{Ca}^{2+}$  currents contribute to neuropathic pain. However, the change in ADP-firing of injured DRG neurons has not been widely studied yet. Here we applied patch clamp to record ADP-firing and T-type  $\text{Ca}^{2+}$  currents in intact and chronically compressed DRG (CCD) neurons and examined T-type  $\text{Ca}^{2+}$  channel proteins expression with western blotting. After CCD injury, the incidences of both ADP firing and non-ADP burst firing increased, and T-type  $\text{Ca}^{2+}$  channels contributed to both of these firing patterns. The neurons discharging large-amplitude-ADP firing were TTX-insensitive, implying that high-density T-type  $\text{Ca}^{2+}$  channels might cooperate with TTX-insensitive  $\text{Na}^+$  channels to reduce the AP threshold. By contrast, the neurons displaying non-ADP burst firing were TTX-sensitive, implying that low density T-type  $\text{Ca}^{2+}$  channels may cooperate with TTX-sensitive  $\text{Na}^+$  channels to increase AP number. In DRG neurons, T-type  $\text{Ca}^{2+}$  currents density varied widely, ranging between 100 pA/pF and 5 pA/pF. After injury, the proportion of DRG neurons with large T-type  $\text{Ca}^{2+}$  currents increased in parallel with the increase in the incidence of large-amplitude-ADP firing. And in addition to Cav3.2, Cav3.3 channels are also likely to contribute to low-threshold firing. The data revealed that T-type  $\text{Ca}^{2+}$  channels may play a dual role in modulating the injured neurons' high excitability through a cooperative process with  $\text{Na}^+$  channels, thereby contributing to neuropathic pain.

## Keywords

T-type  $\text{Ca}^{2+}$  current, afterdepolarizing potential, Cav3.2, neuropathic pain

Date Received: 5 September 2021; Revised 14 September 2022; accepted: 25 September 2022

## Introduction

As low-voltage-activated (LVA)  $\text{Ca}^{2+}$  channels, T-type  $\text{Ca}^{2+}$  channels open at voltages near the resting membrane potential (RMP) and display fast activation and inactivation kinetics.<sup>1</sup> Inward T-type  $\text{Ca}^{2+}$  currents induce prolonged depolarization. Once the depolarization level reaches the threshold potential, plenty of  $\text{Na}^+$  channels are activated and action potential (AP) is generated which is superimposed on the prolonged depolarization. The prolonged depolarization below AP is recorded as afterdepolarizing potentials (ADP). T-type  $\text{Ca}^{2+}$  channels have long been known to play a fundamental role in modulating neural excitability and then to contribute to acute and chronic pain in both the central and peripheral nervous systems (CNS, PNS).<sup>2-4</sup> In various peripheral nerve injuries and diabetic neuropathic pain model

animals, LVA T-type  $\text{Ca}^{2+}$  currents in dorsal root ganglia (DRG) neurons significantly increase, enhancing the excitability of DRG neurons.<sup>2-5</sup> Included in the T-type  $\text{Ca}^{2+}$

<sup>1</sup>Department of Physiology and Pathophysiology, School of Basic Medical Sciences, Xi'an Jiaotong University Health Science Center, Xi'an, China

<sup>2</sup>Clinical Experimental Center, Xi'an International Medical Center Hospital, Xi'an, China

<sup>3</sup>Key Laboratory of Environment and Genes Related to Diseases, Ministry of Education, Xi'an Jiaotong University, Xi'an, China

<sup>4</sup>Institute of Neuroscience, Translational Medicine Institute, Xi'an Jiaotong University Health Science Center, Xi'an, China

## Corresponding Author:

Yuying Wang, Xi'an Jiaotong University, 807, 76 Yan-Ta West Rd, Ke-Jiao Building, Xi'an 710061, China.  
Email: [wangyyzh@xjtu.edu.cn](mailto:wangyyzh@xjtu.edu.cn)



Creative Commons Non Commercial CC BY-NC: This article is distributed under the terms of the Creative Commons Attribution-NonCommercial 4.0 License (<https://creativecommons.org/licenses/by-nc/4.0/>) which permits non-commercial use, reproduction and distribution of the work without further permission provided the original work is attributed as specified on the SAGE

and Open Access pages (<https://us.sagepub.com/en-us/nam/open-access-at-sage>).

channel family are the Cav3.1, Cav3.2, and Cav3.3 channels. In CNS, Cav3.1 and Cav3.2 channels act as pacemaker,<sup>6</sup> whereas Cav3.3 channels induce burst-firing.<sup>7,8</sup> Cav3.2 and Cav3.3 channels are normally expressed in DRG. The Cav3.3 channel expression level is low in DRG, whereas Cav3.2 channels predominate within small and medium-sized neurons.<sup>1,9</sup> Cav3.2 channels are abundant in a subgroup of medium-sized DRG neurons and cause these neurons to discharge low-threshold APs with a characteristic ADP.<sup>5,10-12</sup> Since the ADP is generated by Cav3.2 currents, accordingly, the amplitude of ADP is related to the expression level of Cav3.2 channels. In neuropathic pain, Cav3.2 expression increases at DRG level.<sup>2-5</sup> Thus, the incidence of large-amplitude-ADP firing is most likely to increase. However, we also observed low threshold small-amplitude-ADP firing in injured DRG neurons. Therefore, the association between Cav3.2 channels and low-threshold firing patterns needs to be explored deeply.

Here, we employed chronic compression of DRG rats, a neuropathic pain model, to study the low-threshold firing pattern of compressed DRG neurons in order to reveal the underlying mechanism for the modulation of T-type  $\text{Ca}^{2+}$  channels in low-threshold firing patterns.

## Materials and methods

### Animals

Experiments were performed on young adult male Sprague-Dawley rats (150–200 g) obtained from the Medical Experimental Animal Center of Xi'an Jiaotong University, Shaanxi Province, China. Rats were housed under a standard 12 h light/dark cycle at room temperature with food and water provided *ad libitum*. The experimental protocols were approved by the Institutional Animal Care Committee of Xi'an Jiaotong University and in accordance with ethical guidelines of the International Association for the Study of Pain.<sup>13</sup> All efforts were made to minimize the number of experimental animals and their suffering.

### Chronic compressed dorsal root ganglia (CCD) rat model

The rats were divided into two groups: a CCD group and a sham group. Sham operation animals were anesthetized and the left L4 and L5 intervertebral foramina were exposed, without the insertion of rod.

The animal model employed for DRG compression was reported previously.<sup>14,15</sup> Briefly, the rats were anesthetized with pentobarbital sodium (40 mg/kg, i.p.), the left L4 and L5 intervertebral foramina were exposed, and an L-shaped stainless-steel rod (4 \* 2 mm in length and 0.6 mm in diameter) was inserted into each foramen. A transient twitch of the ipsilateral hind leg muscles of the animal was observed when the DRG was touched by the steel rod. Antibiotic penicillin was administered systemically to both sham and

CCD group for twice at the operation day (100,000 U for each time, i.p.).

### Dorsal root ganglia neurons preparation

Experiments were performed on surface DRG neurons in whole ganglion obtained from CCD and sham-operation rats on day 3–4 post operation. Animals were heavily anesthetized with pentobarbital sodium (55 mg/kg, i.p.) and then decapitated. The left L4 and L5 DRG were rapidly removed and the whole ganglion was placed in a tube containing protease (0.4 mg/mL; Sigma) and collagenase (1 mg/mL; Sigma type 1). The tube was bathed for 30–40 min at 35°C. The course of digestion is very important for later successful electrophysiological recording, because the neuronal surfaces of individual DRG are enveloped by a tight tissue composed of satellite cells. Next the ganglia in the tube were rinsed three times with Hank's balanced salt solution (HBSS) to remove enzymes. Ganglia were kept in oxygenated artificial cerebral spinal fluid (ACSF) (95%  $\text{O}_2$  and 5%  $\text{CO}_2$ ) at 24°C for 1 h. ACSF contains (in mM): 125 NaCl, 3.8 KCl, 1.2  $\text{KH}_2\text{PO}_4$ , 1.0  $\text{MgCl}_2$ , 2.5  $\text{CaCl}_2$ , 25  $\text{NaHCO}_3$ , 10 glucose. At last, single DRG was fixed with a grid of nylon threads glued to a "U"-shaped platinum frame contained in a recording chamber. The chamber was mounted on the stage of an upright microscope (BX51WI; Olympus, Tokyo, Japan) with infrared differential interference contrast optics. During recording, ganglia were kept perfused with oxygenated ACSF.<sup>16</sup>

### Electrophysiological recording

The whole-cell patch-clamp recording was performed at room temperature (22–25°C) on left L4 and L5 DRG neurons from CCD and sham-operated rats using a Multiclamp 700B patch-clamp amplifier (Molecular Devices, Sunnyvale, CA, USA). Patch pipettes (1–3 M $\Omega$ ) were pulled from the borosilicate glass on a puller (p-97, Sutter).

For recording action potentials (APs), recording electrodes having a resistance of 1–3 M $\Omega$  were filled with a physiological solution containing (in mmol/L): 140 KCl, 5 NaCl, 5 Mg-ATP, 1  $\text{MgCl}_2$ , 5 EGTA, 2  $\text{CaCl}_2$ , and 15 HEPES, adjusted to pH 7.4 with KOH. The bath solution contained (in mmol/L): 144 NaCl, 2.5 KCl, 1  $\text{MgCl}_2$ , 2  $\text{CaCl}_2$ , 5 HEPES and 10 mmol/L Glucose, adjusted to pH 7.4 with NaOH.<sup>17</sup>

Patch clamp recordings of T-type  $\text{Ca}^{2+}$  currents were made in the whole-cell configuration. The pipette solution contained: 135 mM CsCl, 1 mM  $\text{MgCl}_2$ , 10 mM EGTA, 10 mM HEPES and 1 mM Mg-ATP with pH adjusted to 7.2 using CsOH. The external solution consisted of 135 mM TEACl, 1 mM  $\text{MgCl}_2$ , 10 mM  $\text{BaCl}_2$ , 10 mM HEPES, and 11 mM glucose, with pH adjusted to 7.4 using TEA-OH. The osmolarity of all pipette solutions and bath solutions were adjusted to roughly 295–305 mOsm/L. Ten  $\mu\text{M}$  of nifedipine and five hundred nM of TTX were delivered to the bath solution on the recording day.<sup>18</sup>

Ramp stimulation applies continuously increasing current or voltage command, so it is convenient to observe threshold potential or clamped voltage. But the slope of ramp stimulation is slow, so it is inconvenient to observe the activation of fast channel. Here we applied both step and ramp commands to record electrophysiological data.

Neurons were subjected to 200-ms step-current commands, from 10 pA to 200 pA in 10 pA increments, to record rheobase. Step-current commands of 500–1000 ms from 1 to 5 times rheobase in increments of 1 \* rheobase or 500–1000 ms ramp-current commands with an intensity of 5 \* rheobase were applied to record neurons' firing patterns.

To record T-type  $\text{Ca}^{2+}$  currents, neurons were held at  $-90$  mV and 250-ms step-voltage commands from  $-90$  to  $+50$  mV were applied in 10 mV increments or 500-ms ramp-voltage commands were applied from  $-90$  to  $+30$  mV. Ramp voltage command clearly separated T-type  $\text{Ca}^{2+}$  currents (LVA  $\text{Ca}^{2+}$  currents) from high voltage activated  $\text{Ca}^{2+}$  currents (HVA  $\text{Ca}^{2+}$  currents) in one trace.

To compare T-type  $\text{Ca}^{2+}$  currents density of neurons between CCD and sham group, step-voltage commands from  $-90$  to  $+50$  mV were applied in 10 mV increments. The amplitude of peak current was measured at  $-40$  mV voltage command and then divided by the cell capacitance of recorded neuron.

Data acquisition was filtered at 10 kHz and sampled at 20 kHz with the Clampex 9.0 software system (Molecular Devices) through the digitizer (Digidata 1322A, Molecular Devices). Membrane properties were monitored with the built-in pCLAMP membrane test. In order to obtain reliable recordings, cells were allowed to equilibrate for 2 min before the start of recording. Neurons with membrane resistance  $\geq 400$  M $\Omega$ , series resistance  $\leq 5$  M $\Omega$ , holding current  $\leq 100$  pA and membrane potential negative than  $-50$  mV were accepted. The series resistance was compensated to above 70%, and capacitance was compensated to above 70%.

The results analysis was carried out by Clampfit 10.4 (Molecular Devices) and OriginPro 8.0 (Originlab Corporation, Northampton, MA, USA).

### Western-blot detection of Cav3.2 and Cav3.3 channels in dorsal root ganglia

We measured Cav3.3 expression in DRG after injury. CCD and sham-operated rats ( $n = 12$  for each group) were sacrificed on day 3 post operation. The left L4 and L5 DRG were then removed rapidly and stored at  $-80^\circ\text{C}$ . Both L4 and L5 DRG from the same animals were pooled together. Next, total protein was extracted and preserved at  $-80^\circ\text{C}$ . The DRGs were homogenized in RIPA lysis buffer (Santa Cruz Biotechnology, USA) with a protease inhibitor cocktail, and then sonicated on ice and centrifuged at 12,000 g for 15 min at  $4^\circ\text{C}$  to isolate the supernatant, which contained the total protein sample. Ten  $\mu\text{g}$  of protein was applied to polyacrylamide gels (10% resolving gels with 4% stacking gels) under reducing conditions using the BioRad MiniProtean III system (Bio-Rad).

After protein concentrations were determined with BCA assays, the protein samples were separated on a 10% SDS-PAGE gels and transferred to polyvinylidene-fluoride (PVDF) membranes (Merck Millipore). After blocking with 3% fat-free dried milk in TBST (20 mM Tris-HCl, 150 mM NaCl, 0.1% Tween 20, pH 7.6) at room temperature for 1 h, PVDF membranes were incubated with mouse anti-Cav3.2 (1:1000, NBP1-22,444ss, Novusbio, Centennial, USA) or mouse anti-Cav3.3 (1:200, Cat#: ACC-009, Alomone Labs, Israel) and anti- $\beta$ -actin (1:1000, Abcam, USA) antibodies in 3% fat-free dried milk in TBST overnight at  $4^\circ\text{C}$ . The blots were then washed with TBST, followed by incubation with (1:4000) horseradish-peroxidase-conjugated, goat anti-mouse antibody (Bio-Rad). Immunoreactive bands were visualized using Renaissance Chemiluminescence Reagent (Millipore, USA). Densitometric analysis was carried out with ImageJ (Bio-Rad, CA, USA, mean grey value). The protein levels of target proteins were normalized to that of  $\beta$ -actin.

### Drugs

Reagents were purchased from Sigma-Aldrich Co. (St Louis, MO, USA).

### Statistical analysis

All values were given as the mean  $\pm$  standard error of the mean (SEM). Statistical significance ( $p < 0.05$ ) was calculated using the t-test for unpaired data or one-way ANOVA using OriginPro 8.0 (Originlab Corporation, Northampton, MA, USA).

### Results

Patch-clamp recording was performed on low-threshold DRG neurons from CCD and sham-operated rats on days 3–4 after surgery. We recorded 65 DRG neurons from the sham group and 65 neurons from the CCD group.

Eighteen neurons from the sham group and 45 neurons from the CCD group exhibited first AP around  $-50$  mV. Injury increased the incidence of low threshold firing (sham group vs. CCD group: 27.69% vs. 69.23%, Chi-square test,  $***p < 0.0001$ ). The APs were considered to be of low threshold since they were recorded near the resting membrane potential.<sup>19</sup> There were no differences in the RMP of low-threshold neurons between the sham and CCD groups (sham group:  $n = 18$ ,  $-56.33 \pm 1.07$  mV; CCD group:  $n = 45$ ,  $-57.40 \pm 0.59$  mV). The tested neurons were classified into small (capacitance: 20–35 pF), medium-sized (capacitance: 40–65 pF) and large cells (capacitance:  $> 70$  pF) on the basis of membrane capacitance.<sup>17</sup> One small and seventeen medium-sized neurons in the sham group and two small and forty-three medium-sized neurons in the CCD group were low-threshold neurons. Most low-threshold neurons were

medium-sized (sham group:  $45.94 \pm 1.22$  pF,  $n = 18$ ; CCD group:  $49.11 \pm 1.45$  pF,  $n = 45$ ).

### **Low-threshold afterdepolarizing potentials firing pattern of dorsal root ganglia neurons**

All 18 neurons from the sham group and 30 neurons from the CCD group generated low-threshold APs followed by prominent ADPs. Injury enhanced ADP-firing (sham group vs. CCD group: 27.69% vs. 46.15%, Chi-square test,  $*p < 0.05$ ). In response to both step and ramp current input, the ADP firing neurons exhibited fast adaptation firing (Figure 1). Among these neurons, 16/18 neurons from the sham group and 18/30 neurons from the CCD group exhibited only single AP. The ADP amplitude was measured in the firing in response to a rheobase intensity of current input. The amplitude of the ADP was  $12.08 \pm 1.39$  mV for the sham group and  $20.19 \pm 2.51$  mV for the CCD group (Figure 1(a), unpaired t-test,  $*p < 0.05$ ). Other 2 neurons from the sham group and 12 neurons from the CCD group discharged burst firing (Figure 1(b)). The amplitude of the ADP was around 10 mV for the sham group and  $10.45 \pm 1.55$  mV for the CCD group (Figure 1(b)). Because there were only 2 neurons in sham group, we didn't test that if the difference between two groups was significant. The amplitude of the ADPs ranged from 3 mV to 40 mV, and there was a tendency for single AP to be present in large-amplitude ADPs, whereas burst firing was associated with small-amplitude ADP. For these neurons displaying ADP, 2 neurons from the sham group and 8 neurons from the CCD group exhibited ADPs with amplitude  $\geq 20$  mV, injury increased the proportion of neurons with large-amplitude ADP (sham group vs. CCD group: 3.08% vs. 12.31%, Chi-square test,  $*p < 0.05$ ). In response to ramp input current, neurons generated ADP-firing when the membrane potential ranged from  $-55$  to  $-40$  mV (Figure 1(c), sham group:  $-47.0 \pm 1.02$  mV,  $n = 18$ ; CCD group:  $-46.37 \pm 0.87$  mV,  $n = 30$ ).

In addition to above ADP-firing, spontaneous repetitive ADP firing was recorded in 4 neurons from the CCD group (Figure 1(d)).

Cav3.2 channels are sensitive to  $\text{NiCl}_2$ .<sup>20</sup> We applied  $\text{NiCl}_2$  to block ADP firing. Application of  $\text{NiCl}_2$  (50–100  $\mu\text{M}$ ) fully blocked ADP firing (Figure 1(e)). For neurons with large-amplitude-ADP firing (ADP amplitude  $\geq 20$  mV), the application of  $\text{NiCl}_2$  significant increased the rheobase from  $32.50 \pm 4.79$  pA to  $317.50 \pm 17.50$  pA ( $n = 4$ ), suggesting that Cav3.2 T-type  $\text{Ca}^{2+}$  currents were chiefly responsible for the low threshold of these neurons.

### **Low-threshold non-afterdepolarizing potentials burst firing pattern of dorsal root ganglia neurons**

As for other 15 low threshold neurons from CCD group, 10/15 neurons generated rapidly adapted burst firing without a

corresponding prominent ADP in response to both step and ramp current inputs (Figure 2(a)). Similar to that of ADP firing neurons in response to ramp input current, the non-ADP burst firing neurons also generated repetitive firing (Figure 2(a)) at potential ranging from  $-50$  to  $-30$  mV (from  $-41.20 \pm 0.90$  mV to  $-33.30 \pm 1.58$  mV,  $n = 10$ ), suggesting that low-voltage-activated T-type  $\text{Ca}^{2+}$  channels contribute to the non-ADP burst firing. The rheobase for the non-ADP burst firing was higher than that of ADP burst firing (Figure 2(a),  $73.00 \pm 7.00$  pA,  $n = 10$ , vs.  $37.67 \pm 2.48$  pA,  $n = 30$ , unpaired t-test,  $****p < 0.0001$ ), implying T-type  $\text{Ca}^{2+}$  channels expression level may be low in neurons with non-ADP burst firing. Other 5/15 low threshold neurons generated a combination of ADP firing and non-ADP burst firing (Figure 2(b)). In response to ramp input current, these neurons generated ADP firing followed by non-ADP repetitive firing (Figure 2(b)) at potential from  $-55$  to  $-30$  mV (from  $-48.0 \pm 3.3$  mV to  $-34.2 \pm 3.8$  mV,  $n = 5$ ).

Hyperpolarization ensured more T-type  $\text{Ca}^{2+}$  channels in a state of non-inactivated. Thus we hyperpolarized the resting membrane potentials (RMPs) to observe changes in rapidly adapted burst firings. Then non-ADP burst firing switched to burst firing with prominent ADP (Figure 2(c)). And hyperpolarization changed combination firing pattern to repetitive burst firing (Figure 2(d)). These changes confirmed that these non-ADP burst firing neurons were distributed with low density of T-type  $\text{Ca}^{2+}$  channels, implying that large T-type  $\text{Ca}^{2+}$  currents contributed to ADP firing whereas small T-type  $\text{Ca}^{2+}$  currents contributed to burst firing.

$\text{NiCl}_2$  (100–200  $\mu\text{M}$ ) inhibited non-ADP burst firing but left the first AP intact (Figure 2(e)), and only slightly increased the rheobase from  $57.50 \pm 8.54$  pA to  $87.50 \pm 12.50$  pA ( $n = 4$ , paired t-test,  $**p < 0.01$ ), suggesting that other ion channels than T-type  $\text{Ca}^{2+}$  channels modulated the threshold of non-ADP burst firing.

### **The role of $\text{Na}^+$ channels in afterdepolarizing potentials firing**

High density of T-type  $\text{Ca}^{2+}$  channels induced large-amplitude-ADP and it corresponded with low threshold. However, we observed that the amplitude of ADP varied widely. Small-ADP or non-ADP firing was also correlated with low-threshold, implying that T-type  $\text{Ca}^{2+}$  currents in combination with  $\text{Na}^+$  currents determined the threshold potential. In response to increasing intensities of step input currents, large-amplitude-ADP ( $\geq 20$  mV) gradually diminished in size to a small amplitude of depolarized potential without an AP above it (Figure 3(a)), implying that the  $\text{Na}^+$  channels of these neurons may be activated at high-voltage and these neurons may be sensitive to both low intensity and high intensity of stimuli.

Two neurons from the sham group and eight neurons from the CCD group exhibited very large ADP (ADP amplitude



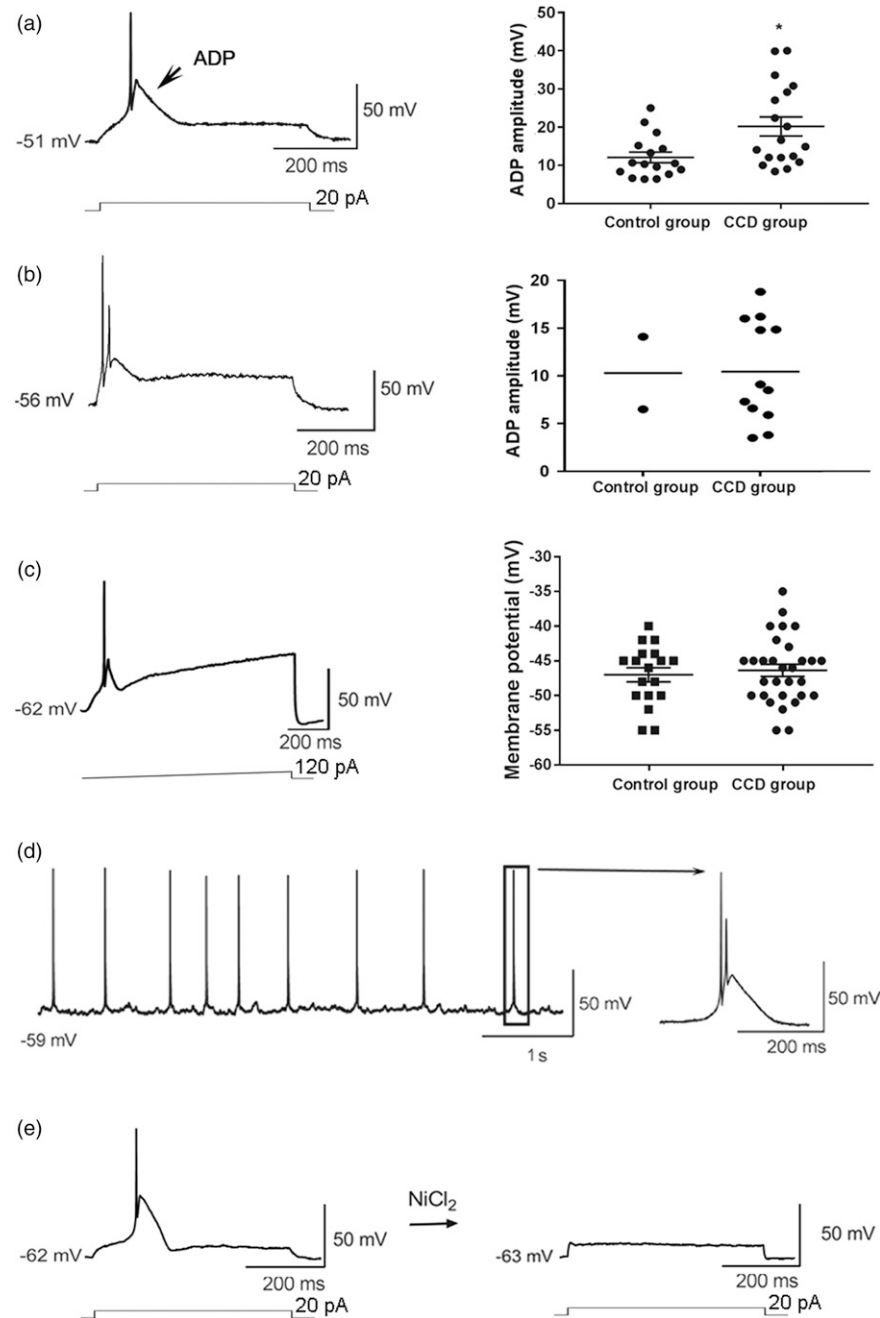


**Figure 1.** Low-threshold ADP-firing of DRG neurons. (a) Representation of single-AP firing with prominent ADP (left panel). ADP amplitudes in single-AP firing were compared between the sham and CCD group (right panel,  $*p < 0.05$ ). Arrow indicates ADP, ADP: afterdepolarizing potential. (b) Representation of burst firing with prominent ADP (left panel). ADP amplitudes in burst firing were compared between the sham and CCD groups (right panel). (c) Representation of ADP-firing in response to ramp current input (left panel). The threshold potentials of AP in response to ramp current were compared between sham group and CCD group (right panel). (d) Representation of spontaneous ADP-firing. The arrow indicates an enlarged single AP. E: Application of 50  $\mu\text{M}$   $\text{NiCl}_2$  blocked ADP firing.

$\geq 20$  mV). Application of tetrodotoxin (TTX) (300 nM) only slightly reduced the amplitude of the AP for these neurons (Figure 3(b)). However, 300 nM TTX fully blocked small-ADP firing and low-threshold non-ADP burst firing (Figure 3(c)).

### T-type $\text{Ca}^{2+}$ current of dorsal root ganglia neurons

T-type  $\text{Ca}^{2+}$  currents were recorded in medium-sized DRG neurons from both sham-operated and CCD rats. Ramp voltage command clearly separated T-type  $\text{Ca}^{2+}$  currents

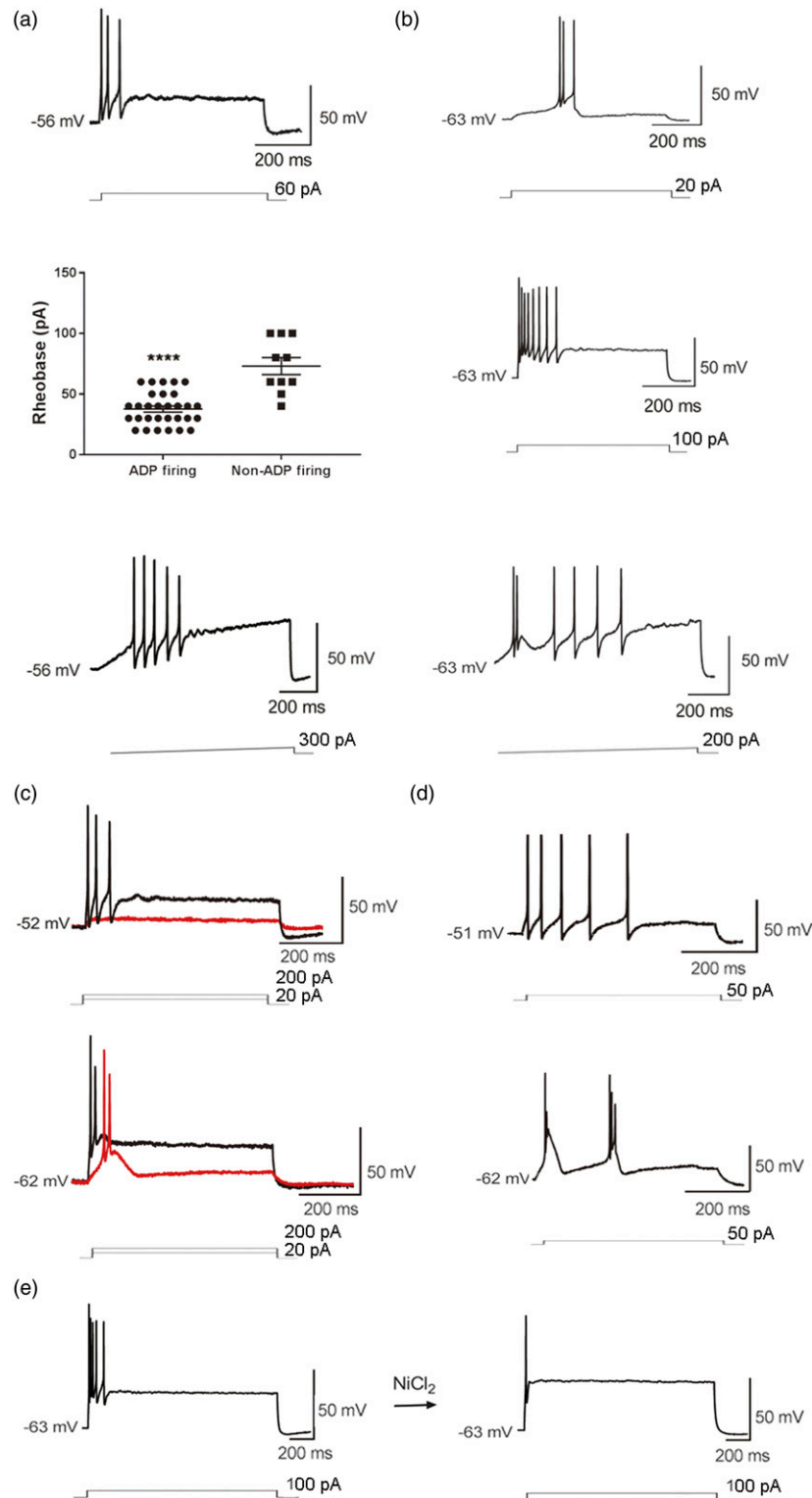


**Figure 2.** Low-threshold non-ADP burst firing of DRG neurons from CCD rats. (a) Representation of non-ADP burst firing in response to step current (upper panel) and ramp current (lower panel). The rheobase of ADP-firing was lower than that of non-ADP-firing (middle panel, \*\*\*\* $p < 0.0001$ ). (b) Combination of ADP-firing and non-ADP burst firing. In response to gradually increasing intensities of current steps, neurons discharged ADP-firing first (upper panel) then a combination firing including ADP firing and non-ADP burst firing (middle panel). In response to a ramp current input, the same neuron exhibited combination firing pattern (lower panel). (c) Non-ADP burst firing (upper panel) switched to ADP burst firing (lower panel) after hyperpolarization of the RMP. (d) Combination firing pattern (upper panel) switched to repetitive ADP firing (lower panel) after hyperpolarization of the RMP. (e) Application of NiCl<sub>2</sub> (100  $\mu$ M) inhibited ADP firing.

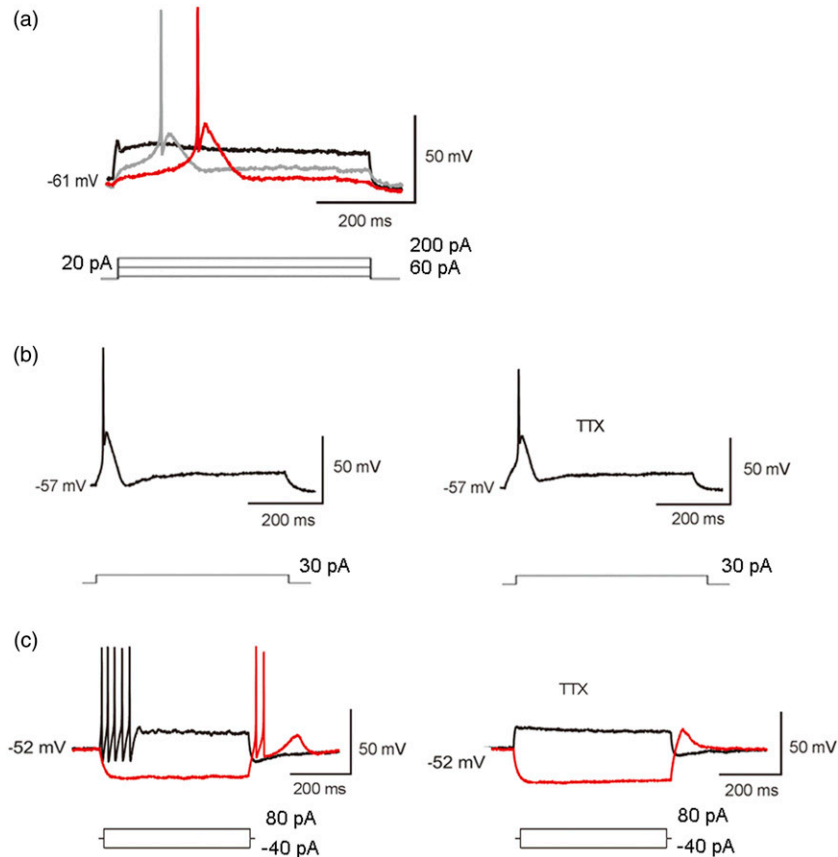


**Figure 3.**  $\text{Na}^+$  channels and ADP/non-ADP firing. (a) Representation of large-amplitude-ADP firing. ADP amplitude gradually decreased in response to increasing intensities of input current. (b) For large-amplitude-ADP firing, the amplitude of the AP was slightly reduced by 300 nM TTX. (c) The APs were fully blocked by 300 nM TTX in non-ADP burst firing, while the post-hyperpolarization rebound APs were also fully blocked by TTX and leave the depolarization potential peak intact.

(LVA  $\text{Ca}^{2+}$  currents) from high voltage activated  $\text{Ca}^{2+}$  currents (HVA  $\text{Ca}^{2+}$  currents). LVA current reached the peak around  $-40$  mV whereas HVA current reached the peak around  $0$  mV.

With ramp voltage clamp recording, 18/60 DRG neurons from the sham group exhibited T-type calcium currents, whereas 28/45 neurons from the CCD group exhibited T-type calcium currents (Figure 4(a)) (sham group vs. CCD group: 30.0% vs. 62.22%, Chi-square test,  $**p < 0.01$ ).

Representative traces of T-type  $\text{Ca}^{2+}$  currents of CCD group neurons recorded with step and ramp-voltage commands are shown in Figure 4(a). In step voltage clamp recording, at  $-40$  mV the T-type  $\text{Ca}^{2+}$  currents peak density varied within a large range from less than  $10$  pA/pF to more than  $80$  pA/pF. After injury the proportion of neurons with large LVA  $\text{Ca}^{2+}$  currents ( $\geq 10$  pA/pF) remarkably increased (sham group vs. CCD group: 8/60 (13.33%) vs. 17/45 (37.78%), Chi-square test,  $**p < 0.01$ ). Neurons exhibited large T-type  $\text{Ca}^{2+}$  current peaks at  $-40$  mV voltage command (Figure 4(b), sham group:  $n = 8$ ,  $48.54 \pm 13.04$  pA/pF; CCD group:  $n = 17$ ,  $52.09 \pm 8.67$  pA/pF). For other neurons, T-type

$\text{Ca}^{2+}$  currents were small (Figure 4(c), sham group:  $n = 10$ ,  $6.35 \pm 0.71$  pA/pF; CCD group:  $n = 11$ ,  $5.67 \pm 0.68$  pA/pF).

### *Cav3.2 and Cav3.3 T-type $\text{Ca}^{2+}$ channels expression in dorsal root ganglia neurons*

In the CNS, Cav3.2 channels act as pacemaker and Cav3.3 channels are associated with burst-firing. Since the occurrences of both ADP-firing and non-ADP burst firing increased in CCD rats, we examined both Cav3.2 and Cav3.3 protein levels in L4 and L5 DRG neurons. Western blotting analysis showed Cav3.2 protein level significantly increased after CCD injury (Figure 4(c), sham group,  $n = 10$ :  $0.700 \pm 0.060$ ; CCD group,  $n = 10$ :  $1.410 \pm 0.070$ , unpaired t-test,  $****p < 0.0001$ ), Cav3.3 expression levels also increased after CCD injury, although overall remained very low. In Figure 4(d), the normalized Cav3.3 expression level was  $0.157 \pm 0.006$  in CCD group ( $n = 12$ ), whereas that was  $0.037 \pm 0.006$  in the sham group ( $n = 12$ , unpaired t-test,  $****p < 0.0001$ ).

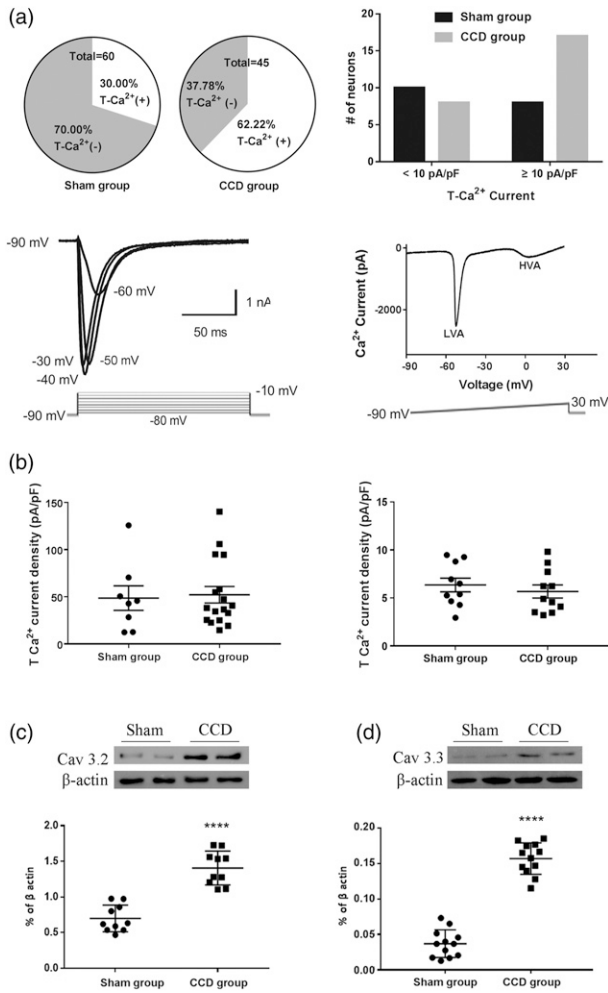


**Figure 4.** T-type  $\text{Ca}^{2+}$  currents of DRG neurons. (a) The distribution of T-type  $\text{Ca}^{2+}$  currents in two groups of DRG neurons (upper panel). T-type  $\text{Ca}^{2+}$  currents recorded in response to step voltage (left panel) and ramp voltage clamps (right panel). LVA: low voltage activated; HVA: high voltage activated. (b) Large ( $\geq 10$  pA/pF) (left panel) and small ( $< 10$  pA/pF) (right panel) T-type  $\text{Ca}^{2+}$  currents recorded at  $-40$  mV command in step voltage clamp were compared between the sham and CCD groups, respectively. (c) Cav3.2 protein expression level of DRG increased in CCD rats. (d) Cav3.3 protein expression level of DRG increased in CCD rats.

## Discussion

It has been reported that T-type calcium channels modulate neuron's excitability and contribute to acute and chronic pain.<sup>4,5,21,22</sup> Both nerve injury and inflammatory mediators increase the expression of T-type  $\text{Ca}^{2+}$  channels in DRG neurons.<sup>23–25</sup> Nerve injury increases the T-type  $\text{Ca}^{2+}$  channels distribution in medium-sized and large DRG neurons.<sup>25</sup> Our electrophysiological data and western blotting results are consistent with this. After CCD injury, the proportion of neurons with T-type  $\text{Ca}^{2+}$  currents increase, meanwhile T-type  $\text{Ca}^{2+}$  channels expression level also increases.

There are three isoforms in T-type  $\text{Ca}^{2+}$  channel family, Cav3.1, Cav3.2 and Cav3.3.<sup>10</sup> In comparison with Cav3.1

and Cav3.3, Cav3.2 has been paid more attention in the research of neuropathic pain for the abundant distribution in nociceptive pathway.<sup>1</sup> After afferent nerve injury, Cav3.2 protein expression was significantly increased in DRG, spinal cord and brain.<sup>2,3,26–28</sup>

The neurons with ADP firing exhibited low rheobase. It is known that Cav3.2  $\text{Ca}^{2+}$  currents underlie ADP.<sup>10–12</sup> Genetic tracing has revealed that Cav3.2 channels are not expressed in slow adapting mechanoreceptors.<sup>29</sup> Coincidentally, ADP-firing displays fast adaptation. ADP amplitude may reflect Cav3.2 T-type  $\text{Ca}^{2+}$  current. Consistently, in the present study, both the incidence of ADP-firing and Cav3.2 expression level increase after CCD injury.

In addition to large-amplitude-ADP firing, the injured neurons also display small-amplitude-ADP firing and low-threshold non-ADP burst firing. Moreover, non-ADP burst firing pattern switched to ADP firing pattern after hyperpolarization of the RMP, indicating that neurons with non-ADP burst firing were distributed with T-type  $\text{Ca}^{2+}$  channels, but the expression level was very low. The rheobase of ADP firing is lower than that of non-ADP burst firing, implying that the density of T-type  $\text{Ca}^{2+}$  channels is critical to the rheobase of neurons. Consistently, the delivery of T-type  $\text{Ca}^{2+}$  channel blocker remarkably increases the rheobase of ADP firing, but only slightly increases the rheobase of non-ADP firing. However, the AP number of non-ADP firing is more than that of ADP firing. So there is a trend that large T-type  $\text{Ca}^{2+}$  currents reduce threshold potential and small T-type  $\text{Ca}^{2+}$  currents contribute to repetitive firing. In the ramp recording, both ADP firing and non-ADP burst firing were only generated within a membrane potential range from  $-55$  mV to  $-30$  mV, implying that the activation of  $\text{Na}^{+}$  currents was dependent on the activation of T-type  $\text{Ca}^{2+}$  currents in response to constant stimulation for these neurons and the threshold potential was determined by the interaction between  $\text{Na}^{+}$  currents and T-type  $\text{Ca}^{2+}$  currents. So, with the contribution of T-type  $\text{Ca}^{2+}$  channels, neurons with high-voltage-activated TTX-insensitive  $\text{Na}^{+}$  channels may be low threshold. Coincidentally, the present study revealed that low-threshold large-amplitude-ADP firing neurons are TTX-insensitive; by contrast, low-threshold small-amplitude-ADP firing and non-ADP burst firing neurons are TTX-sensitive. Firing pattern of injured DRG neurons indicated that after injury the regulation of T-type  $\text{Ca}^{2+}$  channels was associated with  $\text{Na}^{+}$  channels.

In the DRG, T-type  $\text{Ca}^{2+}$  channels are mainly found in small and medium-sized neurons. These neurons are responsible for a variety of sensory modes of signal transmission such as pain, temperature and touch signal. In neuropathic pain models including CCD, the distribution, expression and activation voltage of  $\text{Na}^{+}$  channels are altered among DRG neurons.<sup>30–33</sup> After DRG/nerve injury, TTX-insensitive  $\text{Na}^{+}$  channels expression was downregulated, whereas TTX-sensitive  $\text{Na}^{+}$  channels expression was upregulated.<sup>34</sup> So the expression of T-type  $\text{Ca}^{2+}$  channels may upregulate or downregulate in conjunction with  $\text{Na}^{+}$  channels



to enhance neuronal excitability. Watanabe reported that in inflammatory pain Cav3.2 expression tended to increase in all DRG cells, but drastically increases in TRPV1-positive neurons. And the upregulation may be involved in mechanical hyperalgesia.<sup>35</sup> Consistently, spinal nerve injury significantly increased T-type  $\text{Ca}^{2+}$  current density in small DRG neurons.<sup>25</sup>

Usually high threshold small and medium-sized DRG neurons represent the cell bodies of C and A $\delta$  fiber nociceptors that express both TTX-sensitive and TTX-insensitive  $\text{Na}^+$  channels.<sup>36</sup> The upregulation of T-type  $\text{Ca}^{2+}$  channels density after nerve/DRG injury may significantly reduce the activation potential threshold and enhance the sensitivity of nociceptor neurons to weak nociceptive stimulation or even non-nociceptive stimulation. Then nociceptive signals may be amplified or non-nociceptive signals may be transmitted as nociceptive signals, resulting in hyperalgesia or allodynia. Coincidentally, the blocker of TTX-insensitive Nav1.8 channels attenuated mechanical allodynia.<sup>37</sup> Accordingly, spontaneous ADP firing may be associated with spontaneous pain. In normal, large-amplitude-ADP firing DRG neurons are likely to transmit both nociceptive and non-nociceptive signals.

Different from other neuropathic pain model, Fan et al. found that TTX-insensitive  $\text{Na}^+$  currents also increased in CCD medium-sized DRG neurons.<sup>38</sup> We found more DRG neurons discharged large-amplitude-ADP firing after CCD injury, suggesting both T-type  $\text{Ca}^{2+}$  and TTX-insensitive  $\text{Na}^+$  channels may be increased after CCD injury. So clarifying the change of  $\text{Na}^+$  channel subgroup in each neuron category is necessary in future.

In addition to Cav3.2, DRG neurons also expressed Cav3.3. In CNS, Cav3.3 channels contribute to burst firing. In the present study, compressed DRG neurons also display low-threshold non-ADP burst firing. Cav3.3 channels are not as sensitive to  $\text{NiCl}_2$  as Cav3.2.<sup>20</sup> Meanwhile non-ADP firing was inhibited by higher concentration of  $\text{NiCl}_2$  than ADP firing, indicating non-Cav3.2 (Cav3.3) may contribute to non-ADP firing. The expression of Cav3.3 was very low in our study and other reports.<sup>35,38,39</sup> Yue J et al. reported that Cav3.3 level in DRG significantly increased after spinal injury and may contribute to neuropathic pain.<sup>25</sup> Coincidentally, Wen et al. observed that Cav3.2 and Cav3.3 expression level increased in lumbar spinal cord after CCD injury.<sup>40</sup> Jeub et al. proposed that the upregulation of Cav3.1 or Cav3.3 channels might contribute to the increased T-type  $\text{Ca}^{2+}$  current of DRG neurons in neuropathic pain animal.<sup>27</sup> Consistently, our data showed Cav3.3 expression level in DRG is low but it increased after CCD injury. As for Cav3.1, it is hardly detected in DRG and may not contribute to pain at peripheral nervous system level, but it may play a role in trigeminal neuropathic pain.<sup>41</sup>

Together, the results indicate that collaborations between  $\text{Na}^+$  channels and T-type  $\text{Ca}^{2+}$  channels contribute to low-threshold firing patterns. Thus, large-amplitude-ADP coexists with single AP, whereas small-amplitude-ADP and non-ADP coexist with burst firing. Consistent with the large variation of

ADP amplitude, T-type  $\text{Ca}^{2+}$  current amplitude also varies widely among DRG neurons. Both large and small T-type  $\text{Ca}^{2+}$  currents contribute to elevated neuronal excitability.

## Conclusion

T-type  $\text{Ca}^{2+}$  channels including Cav3.3 may play a dual role in modulating injured neurons' excitability by cooperating with  $\text{Na}^+$  channels, and thereby contribute to neuropathic pain.

## Declaration of conflicting interests

The author(s) declared no potential conflicts of interest with respect to the research, authorship, and/or publication of this article.

## Funding

The author(s) disclosed receipt of the following financial support for the research, authorship, and/or publication of this article: This work was supported by the National Natural Science Foundation of China (grant No. 81300972), Natural Science Foundation of Shaanxi province (grant No. 2020JM-075) and Scientific Research Foundation for Returned Scholars of Ministry of Education.

## ORCID iD

Tong Zhu  <https://orcid.org/0000-0002-1535-9193>

Yuying Wang  <https://orcid.org/0000-0003-0446-2440>

## References

1. Talley EM, Cribbs LL, Lee JH, Daud A, Perez-Reyes E, Bayliss DA. Differential distribution of three members of a gene family encoding low voltage-activated (T-type) calcium channels. *J Neurosci* 1999; 19: 1895–1911.
2. Li Y, Tatsui CE, Rhines LD, North RY, Harrison DS, Cassidy RM, Johansson CA, Kosturakis AK, Edwards DD, Zhang H. Dorsal root ganglion neurons become hyperexcitable and increase expression of voltage-gated T-type calcium channels (Cav3.2) in paclitaxel-induced peripheral neuropathy. *Pain* 2017; 158: 417–429.
3. Liu Q, Chen W, Fan X, Wang J, Fu S, Cui S, Liao F, Cai J, Wang X, Huang Y. Upregulation of interleukin-6 on Cav3.2 T-type calcium channels in dorsal root ganglion neurons contributes to neuropathic pain in rats with spinal nerve ligation. *Exp Neurol* 2019; 317: 226–243.
4. Todorovic SM, Jevtovic-Todorovic V. T-type voltage-gated calcium channels as targets for the development of novel pain therapies. *Br J Pharmacol* 2011; 163: 484–495.
5. Duzhy DE, Viatchenko-Karpinski VY, Khomula EV, Voitenko NV, Belan PV. Upregulation of T-type  $\text{Ca}^{2+}$  channels in long-term diabetes determines increased excitability of a specific type of capsaicin-insensitive DRG neurons. *Mol Pain* 2015; 11: 29.
6. Astori S, Wimmer RD, Prosser HM, Corti C, Corsi M, Liaudet N, Volterra A, Franken P, Adelman JP, Luthi A. The  $\text{Ca}(\text{V})3.3$  calcium channel is the major sleep spindle pacemaker in thalamus. *Proc Natl Acad Sci U S A* 2011; 108: 13823–13828.

7. Cain SM, Snutch TP. T-type calcium channels in burst-firing, network synchrony, and epilepsy. *Biochim Biophys Acta* 2013; 1828: 1572–1578.
8. Monteil A, Chemin J, Bourinet E, Mennessier G, Lory P, Nargeot J. Molecular and functional properties of the human alpha(1G) subunit that forms T-type calcium channels. *J Biol Chem* 2000; 275: 6090–6100.
9. Cardenas CG, Del Mar LP, Scroggs RS. Variation in serotonergic inhibition of calcium channel currents in four types of rat sensory neurons differentiated by membrane properties. *J Neurophysiol* 1995; 74: 1870–1879.
10. Cain SM, Snutch TP. Contributions of T-type calcium channel isoforms to neuronal firing. *Channels (Austin)* 2010; 4: 475–482.
11. Dubreuil AS, Boukhaddaoui H, Desmadryl G, Martinez-Salgado C, Moshourab R, Lewin GR, Carroll P, Valmier J, Scamps F. Role of T-type calcium current in identified D-hair mechanoreceptor neurons studied in vitro. *J Neurosci* 2004; 24: 8480–8484.
12. Jagodic MM, Pathirathna S, Nelson MT, Mancuso S, Joksovic PM, Rosenberg ER, Bayliss DA, Jevtovic-Todorovic V, Todorovic SM. Cell-specific alterations of T-type calcium current in painful diabetic neuropathy enhance excitability of sensory neurons. *J Neurosci* 2007; 27: 3305–3316.
13. Zimmermann M. Ethical guidelines for investigations of experimental pain in conscious animals. *Pain* 1983; 16: 109–110.
14. Hu SJ, Xing JL. An experimental model for chronic compression of dorsal root ganglion produced by intervertebral foramen stenosis in the rat. *Pain* 1998; 77: 15–23.
15. Zhang JM, Song XJ, LaMotte RH. Enhanced excitability of sensory neurons in rats with cutaneous hyperalgesia produced by chronic compression of the dorsal root ganglion. *J Neurophysiol* 1999; 82: 3359–3366.
16. Gong K, Ohara PT, Jasmin L. Patch clamp recordings on intact dorsal root ganglia from adult rats. *J Vis Exp* 2016.
17. Wang Y, Khanna R. Voltage-gated calcium channels are not affected by the novel anti-epileptic drug lacosamide. *Transl Neurosci* 2011; 2: 13–22.
18. Hilliard JK, Sneider TW. Repair methylation of parental DNA in synchronized cultures of Novikoff hepatoma cells. *Nucleic Acids Res* 1975; 2:809–819.
19. Wang Y, Huo F. Inhibition of sympathetic sprouting in CCD rats by lacosamide. *Eur J Pain* 2018; 22: 1641–1650.
20. Lee JH, Gomora JC, Cribbs LL, Perez-Reyes E. Nickel block of three cloned T-type calcium channels: low concentrations selectively block alpha1H. *Biophys J* 1999; 77: 3034–3042.
21. Bourinet E, Zamponi GW. Voltage gated calcium channels as targets for analgesics. *Curr Top Med Chem* 2005; 5: 539–546.
22. Nelson MT, Joksovic PM, Perez-Reyes E, Todorovic SM. The endogenous redox agent L-cysteine induces T-type Ca<sup>2+</sup> channel-dependent sensitization of a novel subpopulation of rat peripheral nociceptors. *J Neurosci* 2005; 25: 8766–8775.
23. Chen YL, Tsaur ML, Wang SW, Wang TY, Hung YC, Lin CS, Chang YF, Wang YC, Shiue SJ, Cheng JK. Chronic intrathecal infusion of mibefradil, ethosuximide and nickel attenuates nerve ligation-induced pain in rats. *Br J Anaesth* 2015; 115: 105–111.
24. Huang D, Liang C, Zhang F, Men H, Du X, Gamper N, Zhang H. Inflammatory mediator bradykinin increases population of sensory neurons expressing functional T-type Ca(2+) channels. *Biochem Biophys Res Commun* 2016; 473: 396–402.
25. Yue J, Liu L, Liu Z, Shu B, Zhang Y. Upregulation of T-type Ca<sup>2+</sup> channels in primary sensory neurons in spinal nerve injury. *Spine (Phila Pa 1976)* 2013; 38: 463–470.
26. Gomez K, Calderon-Rivera A, Sandoval A, Gonzalez-Ramirez R, Vargas-Parada A, Ojeda-Alonso J, Granados-Soto V, Delgado-Lezama R, Felix R. Cdk5-Dependent Phosphorylation of CaV3.2 T-Type Channels: Possible Role in Nerve Ligation-Induced Neuropathic Allodynia and the Compound Action Potential in Primary Afferent C Fibers. *J Neurosci* 2020; 40: 283–296.
27. Jeub M, Taha O, Opitz T, Racz I, Pitsch J, Becker A, Beck H. Partial sciatic nerve ligation leads to an upregulation of Ni(2+)-resistant T-type Ca(2+) currents in capsaicin-responsive nociceptive dorsal root ganglion neurons. *J Pain Res* 2019; 12: 635–647.
28. Shen FY, Chen ZY, Zhong W, Ma LQ, Chen C, Yang ZJ, Xie WL, Wang YW. Alleviation of neuropathic pain by regulating T-type calcium channels in rat anterior cingulate cortex. *Mol Pain* 2015; 11: 7.
29. Bernal Sierra YA, Haseleu J, Kozlenkov A, Begay V, Lewin GR. Genetic Tracing of Cav3.2 T-Type calcium channel expression in the peripheral nervous system. *Front Mol Neurosci* 2017; 10: 70.
30. Eriksson J, Fried K. Expression of the sodium channel transcripts Na(v)1.8 and Na(v)1.9 in injured dorsal root ganglion neurons of interferon-gamma or interferon-gamma receptor deficient mice. *Neurosci Lett* 2003; 338: 242–246.
31. Hong S, Morrow TJ, Paulson PE, Isom LL, Wiley JW. Early painful diabetic neuropathy is associated with differential changes in tetrodotoxin-sensitive and -resistant sodium channels in dorsal root ganglion neurons in the rat. *J Biol Chem* 2004; 279: 29341–29350.
32. Kim DS, Choi JO, Rim HD, Cho HJ. Downregulation of voltage-gated potassium channel alpha gene expression in dorsal root ganglia following chronic constriction injury of the rat sciatic nerve. *Brain Res Mol Brain Res* 2002; 105: 146–152.
33. Song XS, Huang ZJ, Song XJ. Thiamine suppresses thermal hyperalgesia, inhibits hyperexcitability, and lessens alterations of sodium currents in injured, dorsal root ganglion neurons in rats. *Anesthesiology* 2009; 110: 387–400.
34. Yin R, Liu D, Chhoa M, Li CM, Luo Y, Zhang M, Lehto SG, Immke DC, Moyer BD. Voltage-gated sodium channel function and expression in injured and uninjured rat dorsal root ganglia neurons. *Int J Neurosci* 2016; 126: 182–192.
35. Watanabe M, Ueda T, Shibata Y, Kumamoto N, Shimada S, Ugawa S. Expression and regulation of Cav3.2 T-Type calcium channels during inflammatory hyperalgesia in mouse dorsal root ganglion neurons. *PLoS One* 2015; 10: e0127572.
36. Cardenas CG, Del Mar LP, Cooper BY, Scroggs RS. 5HT4 receptors couple positively to tetrodotoxin-insensitive sodium

- channels in a subpopulation of capsaicin-sensitive rat sensory neurons. *J Neurosci* 1997; 17: 7181–7189.
37. Zhang XF, Shieh CC, Chapman ML, Matulenko MA, Hakeem AH, Atkinson RN, Kort ME, Marron BE, Joshi S, Honore P. A-887826 is a structurally novel, potent and voltage-dependent Na(v)1.8 sodium channel blocker that attenuates neuropathic tactile allodynia in rats. *Neuropharmacology* 2010; 59: 201–207.
  38. Fan N, Donnelly DF, LaMotte RH. Chronic compression of mouse dorsal root ganglion alters voltage-gated sodium and potassium currents in medium-sized dorsal root ganglion neurons. *J Neurophysiol* 2011; 106: 3067–3072.
  39. Bourinet E, Alloui A, Monteil A, Barrere C, Couette B, Poirot O, Pages A, McRory J, Snutch TP, Eschalier A. Silencing of the Cav3.2 T-type calcium channel gene in sensory neurons demonstrates its major role in nociception. *EMBO J* 2005; 24: 315–324.
  40. Wen XJ, Xu SY, Chen ZX, Yang CX, Liang H, Li H. The roles of T-type calcium channel in the development of neuropathic pain following chronic compression of rat dorsal root ganglia. *Pharmacology* 2010; 85: 295–300.
  41. Choi S, Yu E, Hwang E, Llinas RR. Pathophysiological implication of CaV3.1 T-type Ca<sup>2+</sup> channels in trigeminal neuropathic pain. *Proc Natl Acad Sci U S A* 2016; 113: 2270–2275.